

Energy Dissipation for Nanometer Sized Acoustic Oscillators

Kuai Yu,¹ Yiqi Jiang,¹ Cameron Wright,² and Gregory V. Hartland^{2*}

¹ *Institute of Microscale Optoelectronics, Shenzhen University, Shenzhen 518060, China*

² *Department of Chemistry and Biochemistry, University of Notre Dame, Notre Dame, Indiana 46556, United States*

Abstract: Ultrafast laser excitation of nanostructures causes rapid heating that can excite vibrational modes that map onto the expansion coordinates. These modes lose energy by radiating sound waves into the environment. Recent experiments have focused on how liquid viscosity and associated viscoelasticity affect the energy dissipation process. In this Perspectives Article we give an overview of the continuum mechanics theory used to describe the damping of the vibrational modes in solid and liquid environments, and describe recent experimental measurements of damping. The theory focuses on the breathing modes of spheres, infinite cylinders and infinite plates, as these are the most relevant to experiments and can be described analytically. We examine the differences between different shapes, and how the relaxation times depends on the dimensions of the nanostructures. In particular, a complicated behavior occurs at sizes where the frequency of the vibrational modes becomes comparable to the relaxation time in the environment. In this regime the quality factors for the breathing modes can be used to estimate environmental relaxation times, providing unique information about the properties of materials at nanoscale dimensions.

* Corresponding author; e-mail: ghartlan@nd.edu

1. Introduction:

A major focus of research in nanoscience has been to explore how size affects the properties of materials. Typically, this is achieved by designing systems and experiments to probe whether nanometer sized objects are different from their bulk counterparts. Perhaps the best known example in physical chemistry is the tunable absorption and emission features of semiconductor nanoparticles that occur when the dimensions of the material are smaller than the exciton Bohr radius.¹⁻³ The spectra of plasmonic Ag and Au nanoparticles also change dramatically with size and shape.⁴⁻⁵ However, this arises from changes in the electric fields at the particle surface created by the incident light beam. Thus, it does not reflect a change in the properties of the material of the particles, and is not a quantum size phenomenon. An exception is for very small metal particles, where electron-surface scattering changes the dielectric function of the material, an effect that was first observed and discussed over 60 years ago!⁶⁻⁷

Recently we and several other groups have explored a situation where the size of the nanostructure changes the *response of the surrounding medium*.⁸⁻¹¹ Normally the properties of the environment around a particle are thought of as being the same of the bulk, modified at close distances by the presence of the interface. However, the acoustic vibrational modes of nanostructures can trigger a viscoelastic response in simple liquids that is not present for macroscale objects.^{9, 12} This occurs because small nanostructures have very high vibrational frequencies, that approach the intrinsic relaxation rates of liquids. In this Perspectives Article we describe the experiments where this effect has been observed, and show how these measurements can be used to obtain information about the properties of the liquid.

We start with the continuum mechanics theory that describes the vibrations of nano-objects, and the transfer of acoustic energy to the environment. Two situations are considered,

first we examine an infinite plate on a solid surface, with and without a spacer layer (which is typically an organic material, such as surfactant or a polymer layer). This is a common experimental situation.¹³⁻¹⁹ The energy relaxation of the plate is simply determined by the acoustic impedances of the different materials,¹³⁻¹⁶ and the damping has a trivial size dependence so that the quality factors for the nanoplate vibrations are independent of size.²⁰⁻²³ We then examine three different types of structures in viscous liquids: spheres,¹¹⁻¹² infinite cylinders,⁹ and infinite plates.¹⁰ The presence of viscosity/viscoelasticity creates a frequency dependent response in the liquid, which means that the liquid behaves differently for different sized structures when the structures have nanometer sized dimensions. Finally, the way liquid relaxation times can be extracted from ultrafast measurements is discussed, along with recent measurements on single nanostructures.¹⁰ We conclude with an outlook on possible applications.

2. Nanoparticle vibrations and damping:

Ultrafast laser excitation of metal or semiconductor nanoparticles causes rapid expansion, that can coherently excite the vibrational modes of the particle that correlate with the expansion coordinate.²⁴⁻³¹ For metal particles this expansion is primarily through lattice heating,²⁵⁻²⁷ whereas, for semiconductors there is also a large effect from the change in the unit cell dimensions that occur upon electronic excitation.³²⁻³³ The frequencies of the modes depend on the size and shape of the particles, and can be accurately calculated using continuum mechanics down to sizes of several hundred atoms,³⁴⁻³⁷ corresponding to dimensions on the order of a few nanometers. Ref. [²⁰] gives a recent review of the vibrational modes nanostructures. The vibrational motion is damped by a combination of internal relaxation (thermoelastic effects) and energy dissipation in

the environment.³⁸ For solid like environments energy dissipation occurs by radiation of sound waves,^{13-16, 20, 23, 39} while for a liquid viscous damping can also play a major role.^{8-12, 40-41}

To calculate the frequencies and damping times for the vibrational modes we start with the equations that describe the displacement/velocity and stress for a solid and for a compressible fluid.¹¹⁻¹² Following Ref. [12], the equations for the displacement \mathbf{u} and stress $\boldsymbol{\sigma}^s$ in the solid are:

$$\rho_s \frac{\partial^2 \mathbf{u}}{\partial t^2} = (2\mu_s + \lambda_s) \nabla^2 \mathbf{u} \quad (1a)$$

$$\boldsymbol{\sigma}^s = \lambda_s (\nabla \cdot \mathbf{u}) \mathbf{I} + \mu_s (\nabla \mathbf{u} + (\nabla \mathbf{u})^T) \quad (1b)$$

where ρ_s is the density of the solid, and μ_s and λ_s are the Lame constants. The equations for velocity \mathbf{v} and stress $\boldsymbol{\sigma}^f$ in the fluid are:

$$\rho_f \frac{\partial \mathbf{v}}{\partial t} = -\nabla p + \beta(\omega) \nabla^2 \mathbf{v} \quad (2a)$$

$$\boldsymbol{\sigma}^f = (-p + \kappa(\omega) (\nabla \cdot \mathbf{v})) \mathbf{I} + 2\eta(\omega) \left(\frac{(\nabla \mathbf{v} + (\nabla \mathbf{v})^T)}{2} - \frac{\nabla \cdot \mathbf{v}}{3} \mathbf{I} \right) \quad (2b)$$

where ρ_f is the fluid density, p is the thermodynamic pressure,¹² and $\beta(\omega) = \kappa(\omega) + 4\eta(\omega)/3$ where $\kappa(\omega)$ and $\eta(\omega)$ are the bulk and shear viscosities of the fluid, which are potentially frequency dependent.⁴² The thermodynamic pressure is related to density fluctuations ρ'_f and speed of sound c_f in the fluid by $p = c_f^2 \rho'_f$.¹¹⁻¹² $\kappa(\omega)$ and $\eta(\omega)$ depend on the compressional and shear relaxation times, λ_{comp} and λ_{sh} . Using a Maxwell model for the fluid, these quantities can be written as $\kappa(\omega) = \tilde{\kappa}/(1 - i\lambda_{\text{comp}}\omega)$ and $\eta(\omega) = \tilde{\eta}/(1 - i\lambda_{\text{sh}}\omega)$ where $\tilde{\kappa}$ and $\tilde{\eta}$ are the regular frequency independent viscosities.^{12, 42} In our analysis we assume that $\lambda_{\text{comp}} = \lambda_{\text{sh}} = \lambda$, so that $\beta(\omega) = \tilde{\beta}/(1 - i\lambda\omega)$ where $\tilde{\beta} = \tilde{\kappa} + 4\tilde{\eta}/3$. The reason for this assumption is that there is not enough information in either the current literature,¹² or the experiments discussed below, to determine separate values of λ_{comp} and λ_{sh} .

Equations (1) and (2) have a relatively simple form for breathing modes, which only involve changes in the radius or thickness of the structure. To solve these equations one has to write out the derivatives in the appropriate coordinate system, and choose functions for the displacement or velocity in the different materials.^{9-12, 39} These functions should match the physics of the problem, that is, they should be oscillating functions for the nanostructure and outgoing waves for the surrounding medium.^{12, 39} Matching the velocity (or displacement) and stress at the surface(s) of the nanostructure then yields an eigenvalue equation which is, of course, different for spheres compared to cylinders or plates. The real part of the solution gives the vibrational frequency, and the imaginary part gives the damping (see the Supporting Information for details). The damping is usually expressed as the quality factor $Q = \omega/2\gamma$ where γ is the damping rate and ω is the angular frequency. In the following we consider two situations that correspond to recent experiments: (i) an infinite nanoplate sitting on a solid substrate with and without a spacer layer,¹⁴⁻¹⁶ and (ii) spheres, infinite cylinders and infinite nanoplates surrounded by a homogeneous liquid.^{9, 12, 39, 43} The ultimate goal is to understand the liquid experiments, but the substrate supported structures provide an important comparison.

2.1. Nanoplates supported on a substrate:

A diagram for an infinite plate (edge lengths much greater than thickness) supported on a solid substrate is shown in Figure 1(a). For this model we choose oscillating functions for the displacement in the plate and spacer layer, and propagating waves for the substrate. The boundary conditions are stress free conditions at the top surface ($z = d + h$), and continuity of displacement and stress at the inner surfaces ($z = d$ and $z = 0$).^{15, 44} This yields five equations that have a non-trivial solution when the determinant of the corresponding matrix is zero (see Supporting

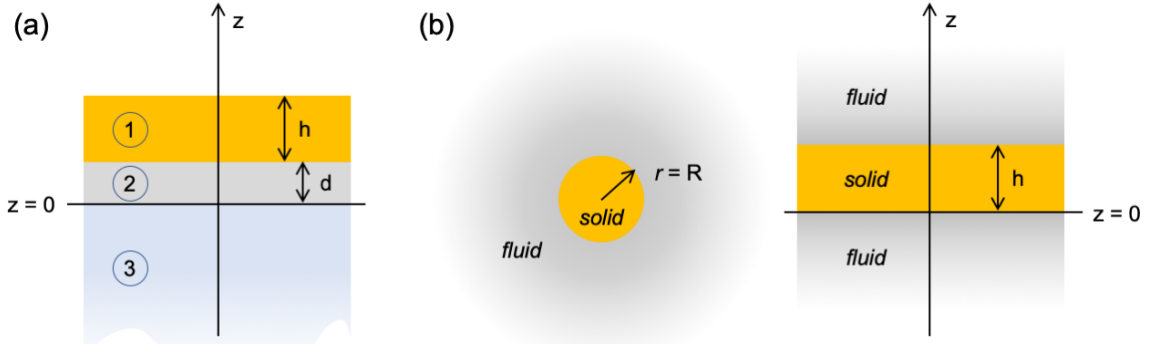


Figure 1: Diagram of (a) substrate supported plates with a spacer layer. h is the thickness of the plate, and d is the thickness of the spacer layer. (b) Spheres and cylinders (left) and plates (right) in a symmetrical liquid environment.

Information for details). After a little manipulation the solution can be written as the following eigenvalue equation:

$$\tan(\xi) \frac{c_1 \rho_1}{c_2 \rho_2} \left(i + \tan \left(\frac{c_1 d}{c_2 h} \xi \right) \frac{c_3 \rho_3}{c_2 \rho_2} \right) + i \tan \left(\frac{c_1 d}{c_2 h} \xi \right) - \frac{c_3 \rho_3}{c_2 \rho_2} = 0 \quad (3)$$

where the eigenvalue $\xi = \omega h / c_1$, and c_i and ρ_i are the longitudinal speeds of sound and densities of the different materials (1 = plate, 2 = spacer layer and 3 = substrate). Note that when $d = 0$ (no spacer layer), this equation reduces to $i c_1 \rho_1 \tan(\xi) - c_3 \rho_3 = 0$, which is the result given in Ref. [15] for a plate on a surface. Also, the properties of the substrate only enter into the eigenvalue equation as the ratio of the acoustic impedances ($Z_i = c_i \rho_i$) of the substrate and spacer layer:

$$Z_3/Z_2 = c_3 \rho_3 / c_2 \rho_2.$$

It is important to note that the nanoplates examined in our experiments have lateral dimensions on the order of several microns and, thus, are strictly not infinite plates. Finite element simulations of the breathing modes for circular plates with different diameter to thickness ratios

(D/h) show that the frequencies are essentially identical to those for an infinite plate for $D/h > 10$, which is satisfied for our samples.

Solving Equation (3) yields the frequency (ν) and quality factor (Q) of the vibration through $\nu = c_1 \text{Re}[\xi]/2\pi h$ and $Q = \text{Re}[\xi]/2\text{Im}[\xi]$. Importantly, there is no explicit frequency or size dependence in Equation (3), besides that through the scaling of the eigenvalue ξ . Thus, the quality factors, which are given by the ratio of the real and imaginary components of ξ , do not depend on size. This means that within this model nanoscale plates on a solid surface behave the same way (have the same quality factors) as macroscale plates with the same d/h ratio. In the following we present results from this analysis in a similar way to that in Ref. [44], where the theory for nanoplate dimers without a substrate was presented and discussed.

Figure 2(a) shows a plot of $\text{Re}[\xi]$ versus the scaled distance d/h for a gold nanoplate on a SiO_2 substrate with a polymer spacer layer. The densities and speeds of sound used in these calculations are $c_1 = 3,240 \text{ m s}^{-1}$ and $\rho_1 = 19,700 \text{ kg m}^{-3}$ for Au, $c_2 = 2,710 \text{ m s}^{-1}$ and $\rho_2 = 1,150 \text{ kg m}^{-3}$ for the polymer, and $c_3 = 5,970 \text{ m s}^{-1}$ and $\rho_3 = 2,200 \text{ kg m}^{-3}$ for SiO_2 . There are a series of modes that correspond to the fundamental, 1st overtone, 2nd overtone etc. of the thickness vibrational modes of the system. Also shown in Figure 2(a) are the eigenvalues for the breathing modes of the free nanoplate ($\xi = n\pi$) and the free spacer layer $\xi = m\pi(c_2/c_1)/(d/h)$ (black dashed lines). At small values of d/h the eigenvalues of the system are very close those of free nanoplates. As d/h increases the eigenvalues undergo a series of avoided crossings.⁴⁴ At certain d/h values the vibrational modes of the system switch from being predominantly nanoplate breathing modes ($\xi = n\pi$), to predominantly thickness vibrations of the spacer layer ($\xi \propto 1/(d/h)$). This change in character occurs at points in the $\text{Re}[\xi]$ versus d/h plot where the eigenvalues for the free nanoplate cross those of the free spacer layer.⁴⁴ Figure 2(b)

shows analogous calculations of $\text{Re}[\xi]$ versus d/h for different substrates: SiO_2 , Si_3N_4 and Au. The $\text{Re}[\xi]$ values for the thickness vibrational modes are relatively insensitive to the substrate except at small spacer layer thicknesses ($d/h < 0.1$), where the higher acoustic impedance substrates cause an increase in frequency (that is, there is an overall stiffening of the system).

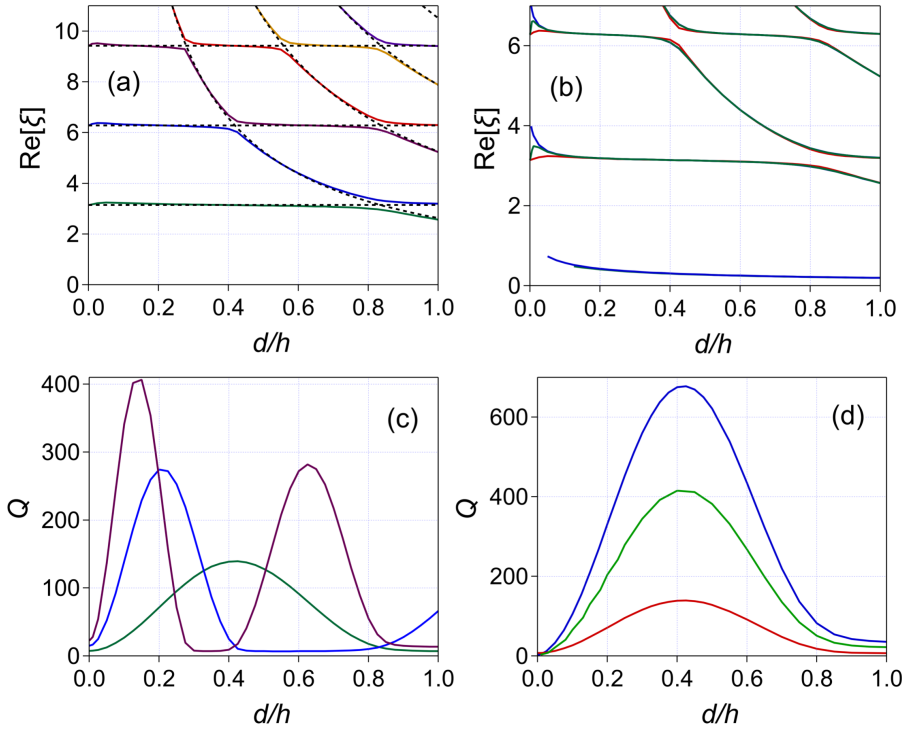


Figure 2: Plots of $\text{Re}[\xi]$ ((a) and (b)) and quality factors Q ((c) and (d)) versus d/h for the thickness vibrational modes of gold plates on different substrates. (a) $\text{Re}[\xi]$ for the first six modes for a SiO_2 substrate. The dashed black lines are the breathing modes of the free nanoplates and the free spacer layer. (b) $\text{Re}[\xi]$ for different substrates over a smaller range: red = SiO_2 , green = Si_3N_4 and blue = Au. (c) Q values for the first three modes for a SiO_2 substrate. (d) Q values for the fundamental breathing mode for different substrates. The colors in panels (c) and (d) match those in panels (a) and (b), respectively.

The calculated quality factors for the first three modes for the SiO_2 substrate are presented in Figure 2(c). There are several points to note from this Figure. First, in general the quality factors increase as the mode frequencies increase. This occurs because the damping rate is similar for the different modes and $Q = \omega/2\gamma$. The second important point is that at small values of d/h , the quality factor increases as d/h increases. In this regime separating the nanoplate from the substrate by a thin polymer layer reduces the damping. This effect was recently observed and analyzed by Hettich et al. in experiments with gold films separated from a substrate by self-assembled molecular layers.^{14, 16} The calculations also show that as the thickness of the spacer layer is increased, the quality factors go through a maximum that occurs at different d/h values for the different modes. Comparison to Figure 2(a) shows that the maxima occur in the flat regions of the $\text{Re}[\xi]$ versus d/h curves, where the vibrational modes have the character of the free nanoplate breathing modes. The quality factors are greatly reduced in the regions where $\xi \propto 1/(d/h)$, i.e., where the vibrational modes take on the character of the spacer layer breathing modes. This occurs because the spacer layer modes suffer strong damping, due to the small difference in the acoustic impedance of the polymer and silica.¹³

A low frequency mode is also seen in Figure 2(b) for the Si_3N_4 and Au substrates. This mode is assigned to motion of the nanoplate relative to the substrate,⁴⁴ and is predicted to be heavily damped. For example, at $d/h = 0.5$ the quality factors for this mode for the Si_3N_4 and Au substrates are $Q_{\text{Si}_3\text{N}_4} \approx 2.09$ and $Q_{\text{Au}} \approx 3.46$. The relative mode also occurs for the SiO_2 substrate. However, we have only included modes with $Q > 1$ in the figures, and for SiO_2 this only occurs at $d/h > 1.3$. In contrast to the small effects for $\text{Re}[\xi]$, the quality factors for the nanoplate vibrations presented in Figure 2(d) show large differences for the different substrates.

The damping is greatly reduced for the higher acoustic impedance substrates, where there are larger differences in acoustic impedance between the spacer layer and the substrate.

The analysis in Figure 2 shows that the thickness of the spacer layer, and the difference in acoustic impedance of the spacer layer and substrate play important roles in the damping of the nanoplate thickness vibrational modes. For a SiO_2 substrate (which is the most thoroughly examined system experimentally) the calculations predict $Q = 7.52$ for no spacer layer ($d/h = 0$).¹⁵ However, such small Q values are typically not seen in experiments. In a recent study we found a value of $Q = 10 \pm 3$ for nanoplates synthesized with PVP as a stabilizing agent.¹⁷ This Q value implies a spacer layer thickness of ~ 1 nm (assuming that the spacer layer has the same acoustic impedance of bulk polymer), which is consistent with the expected thickness of the polymer layer surrounding the nanoplates. It is important to note that in this model the quality factors and (and $\text{Re}[\xi]$) only depend on the value of d/h , not the absolute values of d or h . This is the normal result when the damping of the acoustic modes is controlled by radiation of sound waves into a solid-like environment.^{15, 23}

2.2. Nanostructures in viscous and viscoelastic liquids

We now turn our attention to nanostructures immersed in liquids. Liquid damping experiments have been performed on a variety of samples, including nanospheres and nanorods (both single particle and ensemble experiments),^{8, 11, 40} suspended and supported nanowires,^{9, 39, 45} and suspended nanoplates.¹⁰ To interpret the results, and consequently obtain information about the properties of the liquid, the experiments must be compared to theory. Relatively simple expressions have been derived for the breathing modes of high symmetry structures (spheres, infinite cylinders and infinite plates) in a homogeneous environment.⁹⁻¹² However, the theory is

much more complicated for nanostructures on a substrate, or for vibrational modes that produce shear in the liquid (such as the extensional modes of nanorods).^{9, 43, 46-47} For these reasons we concentrate on the breathing modes of suspended spheres, infinite cylinders and infinite plates.

Figure 1(b) shows a schematic diagram of a sphere/cylinder or infinite plate in a homogeneous liquid. For spheres the displacement in the particle is taken to be a spherical Bessel function of the first kind $j_1(k_s r)$, and an outgoing spherical wave $e^{ik_f r}/r$ is used for the medium.¹¹⁻¹² For cylinders the choices are Bessel functions $J_1(x)$ and Hankel functions $H_1(x)$ of the first kind for the particle and medium, respectively.^{9, 39} For plates sine and cosine terms are used for the particle, and the displacement in the medium is modeled as an outgoing plane wave, either $e^{ik_f z}$ or $e^{-ik_f z}$ depending on the direction.¹⁰ The boundary conditions are now continuity of velocity and stress at the interfaces between the particle and fluid (which are at $r = R$ for the spheres and cylinders, and $z = 0$ and $z = h$ for the plates).^{9-12, 39} This yields a set of equations that can be solved by setting the determinants of the corresponding matrices to zero, see Refs. [¹⁰⁻¹²] and the Supporting Information for details. The results for the different cases are:

$$\text{Spheres: } 4 \frac{c_t^2}{c_l^2} + \frac{4i\omega\eta(\omega)}{c_l^2\rho_s} + \frac{\rho_f}{\rho_s(1 - ik_f(\omega)R)} k_s^2 R^2 - k_s R \frac{j_0(k_s R)}{j_1(k_s R)} = 0 \quad (4a)$$

$$\text{Cylinders: } 2 \frac{c_t^2}{c_l^2} + \frac{2i\omega\eta(\omega)}{c_l^2\rho_s} + \frac{(c_f^2\rho_f - i\omega\beta(\omega))}{c_l^2\rho_s} k_f(\omega)R \frac{H_0(k_f(\omega)R)}{H_1(k_f(\omega)R)} - k_s R \frac{J_0(k_s R)}{J_1(k_s R)} = 0 \quad (4b)$$

$$\text{Plates: } c_l^2\rho_s^2 + \rho_f(c_f^2\rho_f - i\omega\beta(\omega)) + 2ic_l\rho_s \sqrt{\rho_f(c_f^2\rho_f - i\omega\beta(\omega))} \cot(k_s h) = 0 \quad (4c)$$

where $j_i(x)$, $J_i(x)$ and $H_i(x)$ are spherical Bessel functions, Bessel functions and Hankel functions of the first kind, respectively, c_l and c_t are the longitudinal and transverse speeds of sound in the solid, $k_s = \omega/c_l$ and $k_f(\omega) = \frac{\omega}{c_f \sqrt{1-i\omega\beta(\omega)/c_f^2\rho_f}}$.¹² Solution of the above equations gives a complex frequency $\tilde{\omega}$, and the quality factor for the vibrational modes of the nanostructure are given by $Q_{liq} = \text{Re}[\tilde{\omega}]/2\text{Im}[\tilde{\omega}]$ (the “*liq*” subscript emphasizes that damping is due to dissipation of acoustic energy into the surrounding liquid).

The quality factors for spheres, cylinders and plates in water and glycerol are plotted versus the frequency in Figure 3 for water (Fig. 3(a)) and glycerol (Fig. 3(b)). The solid lines show the results using the full viscoelastic calculations, and the dashed lines are for an inviscid liquid ($\tilde{\kappa} = \tilde{\eta} = 0$). The viscosities and liquid relaxation times needed for the viscoelastic calculations were taken from Ref. [¹²]. The simulations show that at low frequencies both models for the liquid give identical quality factors, and a frequency independent response. This occurs because the viscosity terms in Equations 4(a) – (c) are multiplied by ω . Thus, for $\omega \rightarrow 0$ the equations reduce to the corresponding expressions for spheres, cylinders or plates in a solid-like environment, where damping is simply determined by the acoustic impedances of the particle and the surroundings (see the Supporting Information for details).

As the vibrational frequency increases viscosity becomes important, and the quality factors start to decrease due to viscous damping. However, when the vibrational frequencies approach the relaxation rate of the liquid ($\lambda\omega \approx 1$), the Q values start to flatten off, and reach a limiting value for $\lambda\omega \gg 1$. This occurs because at high frequencies the liquid cannot respond to the vibrational motion of the nanostructure.^{9, 11, 42} Thus, the viscoelastic model predicts frequency independent quality factors at low frequencies where viscosity is unimportant, and at high frequencies where the vibrational period is much shorter than the liquid relaxation time. Note that

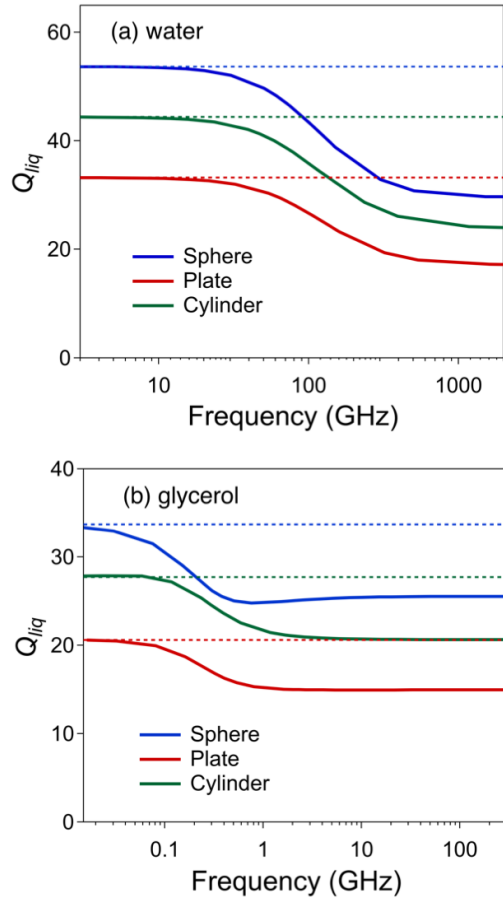


Figure 3: Quality factor for liquid damping Q_{liq} versus frequency for spheres (blue), cylinders (green) and plates (red) in (a) water and (b) glycerol. The dashed lines show results for an inviscid fluid (no viscosity) and the full lines are for a viscoelastic fluid.

the dimensionless parameter $\lambda\omega$ is often referred to as the Deborah number D for the system.^{9, 11,}

⁴² In general a system is considered to behave like a solid when $D \gg 1$, and a liquid for $D \leq 1$.^{9,}

^{11, 42}

The calculations presented in Figure 3 show that spheres give the largest quality factors, and also have the largest change in quality factor with frequency. This means that performing experiments with spheres offers the best opportunity to observe viscoelastic effects and, thus,

measure liquid relaxation times.¹¹ Clearly to interrogate viscoelastic effects experiments should be performed for $\lambda\omega \gg 1$, where there are clear differences between the inviscid and viscoelastic liquid models. However, this is experimentally challenging as it requires ultrafast, preferably single particle measurements, on very small structures (dimensions on the order of 10 nm).

3. Measuring liquid relaxation times from experiments:

The results in Section 2 provide continuum mechanics expressions for how the environment affects energy dissipation for nanometer sized acoustic oscillators. In real systems the measured quality factors also contain contributions from the intrinsic damping from the material of the particle⁴⁰⁻⁴¹ and, for ensemble experiments, inhomogeneous effects from the distribution of sizes and shapes in the sample.^{8, 11} Thus, the total quality factor is given by

$$\frac{1}{Q} = \frac{1}{Q_0} + \frac{1}{Q_{env}} \quad (8)$$

where Q_0 contains the intrinsic damping contributions and/or size distribution effects, and Q_{env} accounts for energy dissipation into the environment. Therefore, to measure Q_{env} the intrinsic damping/size distribution effects have to be determined.

For single particle studies of liquid damping this can be done by recording data for nanostructures with and without a surrounding fluid.^{39, 45} Examples of these measurements for suspended Au nanoplates are presented in Figure 4.¹⁰ The panels on the left show transient absorption traces for three different nanoplates in air, and the corresponding traces for the nanoplates in liquids are shown on the right. The high frequency oscillations in the transient absorption data in Figure 4 are from the breathing mode of the nanoplates. Adding liquid to the system significantly increases the damping of the breathing mode, and the difference between the quality factors for the nanoplates in air and liquid gives $Q_{env} = Q_{liq}$. A lower frequency

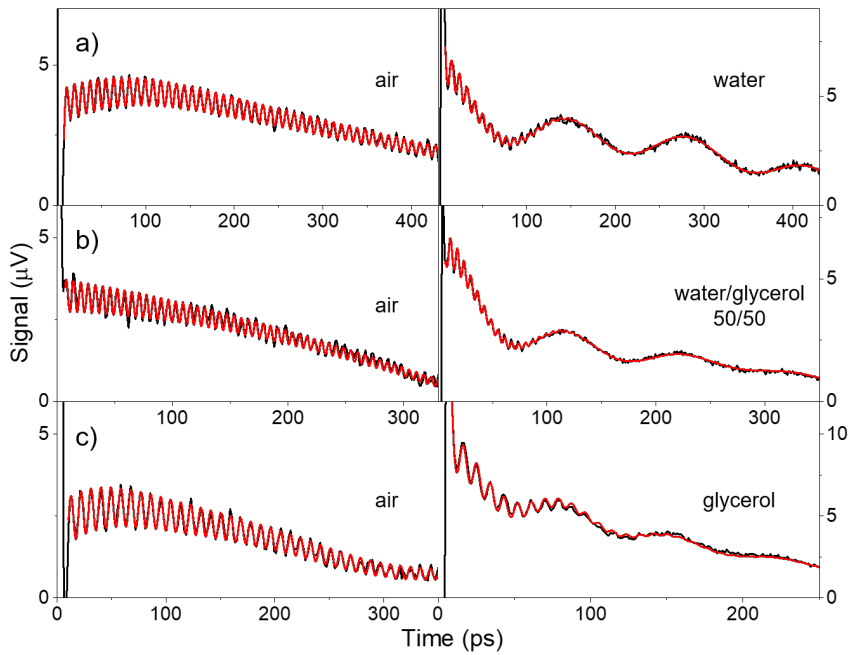


Figure 4: Transient absorption traces of single suspended Au nanoplates in different environments: (a) air and water, (b) air and a 50/50 water/glycerol mixture, (c) air and glycerol. The red lines are fits to the experimental data. The high frequency oscillations are the breathing modes of the plates and the low frequency oscillations in the liquid experiments are Brillouin oscillations. Reprinted with permission from *ACS Nano* **2021**, *15*, 1833-1840. Copyright 2021 American Chemical Society.

oscillation also appears in the liquid experiments. This signal is assigned to Brillouin oscillations in the liquid.¹⁰ Brillouin oscillations are an interference effect caused by reflection of the probe beam from the nanoplates and from sound waves in the liquid that are generated by ultrafast excitation of the nanoplates. For normal incidence the Brillouin oscillation frequency is $f_B = 2c_f n_f / \lambda_{pr}$, where c_f and n_f are the speed of sound and refractive index of the fluid, and λ_{pr} is the probe wavelength.⁴⁸ Note that the presence of Brillouin oscillations can complicate analysis of the breathing modes when the two frequencies are similar.⁴⁹⁻⁵⁰ However, these two signals can be

differentiated by changing the probe laser wavelength.⁵¹⁻⁵² The frequency of the Brillouin oscillations can also provide information about the viscoelastic properties of the liquid,^{10, 51-52} but in this Perspectives article we focus on measuring liquid relaxation times through the damping of the breathing modes.

Figure 5(a) shows plots of the calculated quality factors versus frequency for gold nanoplates in a viscoelastic liquid (solid lines) and inviscid liquid (dashed lines). The markers show the average values of Q_{liq} from the experimental measurements, where the error bars are standard deviations. Comparison to the continuum mechanics calculations shows that the viscoelastic fluid model gives a much better description of the experimental data for both water and glycerol than the simple inviscid model that ignores viscosity. This is a clear demonstration that viscoelastic effects are important for the high frequency vibrational modes of Au nanoplates in simple liquids.^{8, 10-11}

Ensemble measurements for spherical and bipyramidal Au nanoparticles have also shown that viscoelastic effects are needed to correctly describe vibrational damping in viscous liquids.^{8, 11, 46} However, single particle measurements for suspended Au nanowires could be explained simply by radiation of sound waves in the surrounding liquid (the inviscid fluid model).^{22, 43, 45} This shows the difficulty in probing fluid viscoelasticity through vibrational damping measurements. To do this accurately high frequency acoustic oscillators with large intrinsic quality factors are needed. Chemically synthesized Au nanoplates are an excellent system for this, as they can be made with widths on the order of 10 – 20 nm, corresponding to breathing mode frequencies of 80 – 160 GHz, and they have large intrinsic quality factors (typically > 100).^{10, 17-18}

Another way of interpreting the data in Figures 4 and 5(a) is to use the experimental values of Q_{liq} to estimate the relaxation times for the liquids. The relaxation times from this analysis for

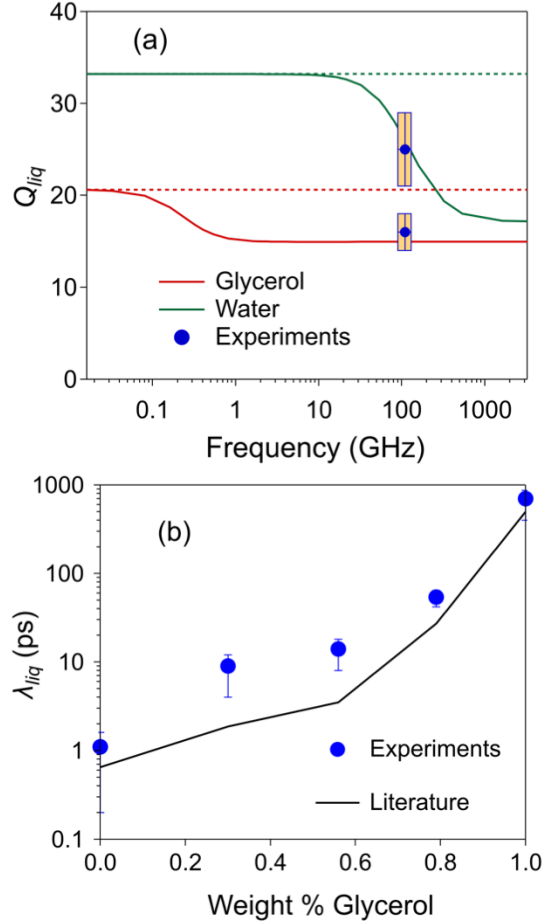


Figure 5: (a) Quality factors Q_{liq} versus frequency for Au nanoplates in water and glycerol. The dashed and solid lines correspond to the inviscid and viscoelastic fluid models, respectively, and the symbols show the experimental data (errors are standard deviations). (b) Liquid relaxation times, λ_{liq} , determined from the experiments. The line shows the relaxation times from Ref. [12]. The experimental data was taken from Ref. [10].

the Au nanoplates are plotted against the weight percentages of glycerol in water in Figure 5(b).¹⁰ The relaxation times vary from a picosecond for water to just under a nanosecond for glycerol. The solid line shows the literature values from Ref. [12], which are in reasonable agreement with the experimental data. Thus, the acoustic mode damping experiments can provide reliable

estimates of liquid relaxation times. The drawback for these measurements is the relatively large errors, which arise from two effects. First, we need to subtract two sets of measurements to determine Q_{liq} , and the errors from the two measurements add for the final value. Second, the Q_{liq} values are not very sensitive to viscosity and the liquid relaxation time. For example, Q_{liq} changes by about a factor of two for water compared to glycerol, whereas, the relaxation times change by almost 3 orders of magnitude. This necessarily means a large uncertainty in the relaxation times determined from Q_{liq} measurements.

4. Summary and Outlook:

Ultrafast laser irradiation of metal nanostructures excites symmetric vibrational modes of the structures that correspond to changes in size. When the nanostructures are in a solid environment, or supported on a surface, these modes lose energy by radiation of sound waves into the environment.^{20-22, 28} The efficiency of this process depends on the difference in acoustic impedance between the nanostructure and the surroundings. The energy dissipation rates can be manipulated by adding a spacer between the nanoplate and the surface, but the quality factors do not depend on the size: nanoscale objects show the same relaxation behavior as macroscale objects.^{13, 15, 20, 23, 39}

In contrast, for a liquid environment the response of the liquid depends on the frequency of the vibrational motion and vibrational profile.^{8, 10-12} At large sizes (low vibrational frequencies) relaxation is simply determined by the acoustic impedance of the liquid. As the size decreases, and the corresponding vibrational frequencies increase, viscosity effects become important and the vibrational quality factors start to decrease. Finally, when the period of the vibrational motion is faster than the liquid relaxation time, the quality factors reach a plateau, which is the signature of

a viscoelastic response in the liquid. In this high frequency limit the liquid has an inviscid solid-like response, with an increased acoustic impedance compared to the low frequency regime. Thus, the response of the liquid to the vibrational motion depends on the size of the nano-object.

The presence of viscoelastic effects in nanoparticle-fluid interactions is now well established in experiments. It has been observed for the high frequency breathing mode vibrations of nanoplates (discussed in detail above),¹⁰ and nanospheres,¹¹ and also for the extensional modes of nano-bipyramids.⁸ These experiments are challenging, because they require accurate quality factor measurements, as well as a procedure for separating intrinsic damping from environmental effects. In single particle measurements this can be done by performing experiments on the same nanostructure with and without a surrounding liquid.

Beyond demonstrating that viscoelastic effects occur in simple liquids, ultrafast measurements provide a way of measuring liquid relaxation times. Because the relaxation times are obtained by comparison to theory, the experiments need to be done on a system that can be accurately modeled. Theories have been presented for the breathing modes of spheres,¹² infinite rods,⁹ and nanoplates suspended in a liquid.¹⁰ These systems have simple boundary conditions of continuity of displacement/velocity and stress at the different interfaces. The extension to supported nanoplates should also be possible. Theories have also been presented for the extensional modes of nanorods, although the boundary conditions are more complicated in this case.^{8-9, 46-47} Note that it is also possible to use acoustic mode damping experiments to study relaxation in solid materials.^{14, 16} However, the way the relaxation time is introduced into the material's properties is very different for solids compared to liquids.¹⁶ Thus, ultrafast measurements in combination with continuum mechanics analysis have the potential to provide new information about soft materials. Importantly, when implemented with single particle

detection, these experiments offer the intriguing possibility of interrogating liquid properties with tens of nanometers spatial resolution.

Supporting Information: The Supporting Information for this paper contains details for the derivation of the eigenvalue equations for nanoplates on a surface, as well as those for spheres cylinder and plates in viscoelastic liquids.

Acknowledgements:

KY and YJ acknowledge the support of the National Natural Science Foundation of China (grant 12074266), the Science and Technology Project of Shenzhen (grant 20200802180159001). GVH and CW acknowledge the support of the National Science Foundation through award CHE-2002300.

References:

1. Murray, C. B.; Norris, D. J.; Bawendi, M. G., Synthesis and Characterization of Nearly Monodisperse Cde (E = S, Se, Te) Semiconductor Nanocrystallites. *J. Am. Chem. Soc.* **1993**, *115*, 8706-8715.
2. Bruchez, M.; Moronne, M.; Gin, P.; Weiss, S.; Alivisatos, A. P., Semiconductor Nanocrystals as Fluorescent Biological Labels. *Science* **1998**, *281*, 2013-2016.
3. Protesescu, L.; Yakunin, S.; Bodnarchuk, M. I.; Krieg, F.; Caputo, R.; Hendon, C. H.; Yang, R. X.; Walsh, A.; Kovalenko, M. V., Nanocrystals of Cesium Lead Halide Perovskites

- (Cspbx3, X = Cl, Br, and I): Novel Optoelectronic Materials Showing Bright Emission with Wide Color Gamut. *Nano Letters* **2015**, *15*, 3692-3696.
4. Kelly, K. L.; Coronado, E.; Zhao, L. L.; Schatz, G. C., The Optical Properties of Metal Nanoparticles: The Influence of Size, Shape, and Dielectric Environment. *J. Phys. Chem. B* **2003**, *107*, 668-677.
 5. Lu, X. M.; Rycenga, M.; Skrabalak, S. E.; Wiley, B.; Xia, Y. N., Chemical Synthesis of Novel Plasmonic Nanoparticles. *Ann. Rev. Phys. Chem.* **2009**, *60*, 167-192.
 6. Fragstein, C. v.; Römer, H., Über Die Anomalie Der Optischen Konstanten. *Zeitschrift für Physik* **1958**, *151*, 54-71.
 7. Hampe, W., Beitrag Zur Deutung Der Anomalen Optischen Eigenschaften Feinstteiliger Metallkolloide in Großer Konzentration. *Zeitschrift für Physik* **1958**, *152*, 476-494.
 8. Pelton, M.; Chakraborty, D.; Malachosky, E.; Guyot-Sionnest, P.; Sader, J. E., Viscoelastic Flows in Simple Liquids Generated by Vibrating Nanostructures. *Phys. Rev. Lett.* **2013**, *111*, 244502.
 9. Chakraborty, D.; Hartland, G. V.; Pelton, M.; Sader, J. E., When Can the Elastic Properties of Simple Liquids Be Probed Using High-Frequency Nanoparticle Vibrations? *J. Phys. Chem. C* **2017**, *122*, 13347-13353.
 10. Yu, K.; Yang, Y.; Wang, J.; Hartland, G. V.; Wang, G. P., Nanoparticle–Fluid Interactions at Ultrahigh Acoustic Vibration Frequencies Studied by Femtosecond Time-Resolved Microscopy. *ACS Nano* **2021**, *15*, 1833-1840.
 11. Uthe, B.; Collis, J. F.; Madadi, M.; Sader, J. E.; Pelton, M., Highly Spherical Nanoparticles Probe Gigahertz Viscoelastic Flows of Simple Liquids without the No-Slip Condition. *J. Phys. Chem. Lett.* **2021**, 4440-4446.

12. Galstyan, V.; Pak, O. S.; Stone, H. A., A Note on the Breathing Mode of an Elastic Sphere in Newtonian and Complex Fluids. *Phys. Fluids* **2015**, *27*, 032001.
13. Marty, R.; Arbouet, A.; Girard, C.; Mlayah, A.; Paillard, V.; Lin, V. K.; Teo, S. L.; Tripathy, S., Damping of the Acoustic Vibrations of Individual Gold Nanoparticles. *Nano Letters* **2011**, *11*, 3301-3306.
14. Hettich, M.; Bruchhausen, A.; Riedel, S.; Geldhauser, T.; Verleger, S.; Issenmann, D.; Ristow, O.; Chauhan, R.; Dual, J.; Erbe, A., et al., Modification of Vibrational Damping Times in Thin Gold Films by Self-Assembled Molecular Layers. *Appl. Phys. Lett.* **2011**, *98*, 261908.
15. Fedou, J.; Viarbitskaya, S.; Marty, R.; Sharma, J.; Paillard, V.; Dujardin, E.; Arbouet, A., From Patterned Optical near-Fields to High Symmetry Acoustic Vibrations in Gold Crystalline Platelets. *Phys. Chem. Chem. Phys.* **2013**, *15*, 4205-4213.
16. Hettich, M.; Jacob, K.; Ristow, O.; Schubert, M.; Bruchhausen, A.; Gusev, V.; Dekorsy, T., Viscoelastic Properties and Efficient Acoustic Damping in Confined Polymer Nano-Layers at Ghz Frequencies. *Scientific Reports* **2016**, *6*, 33471.
17. Wang, J.; Yu, K.; Yang, Y.; Hartland, G. V.; Sader, J. E.; Wang, G. P., Strong Vibrational Coupling in Room Temperature Plasmonic Resonators. *Nature Communications* **2019**, *10*, 1527.
18. Wang, J.; Yang, Y.; Wang, N.; Yu, K.; Hartland, G. V.; Wang, G. P., Long Lifetime and Coupling of Acoustic Vibrations of Gold Nanoplates on Unsupported Thin Films. *J. Phys. Chem. A* **2019**, *123*, 10339-10346.
19. Wang, J.; Li, M.; Jiang, Y.; Yu, K.; Hartland, G. V.; Wang, G. P., Polymer Dependent Acoustic Mode Coupling and Hooke's Law Spring Constants in Stacked Gold Nanoplates. *J. Chem. Phys.* **2021**, *155*, 144701.

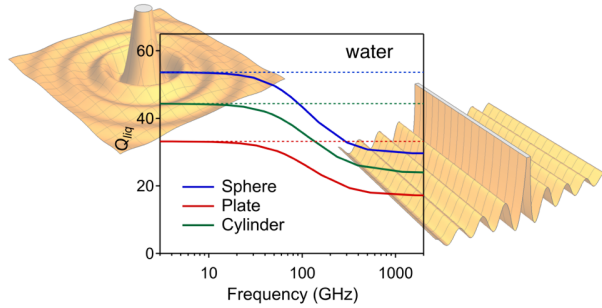
20. Crut, A.; Maioli, P.; Del Fatti, N.; Vallee, F., Acoustic Vibrations of Metal Nano-Objects: Time-Domain Investigations. *Phys. Rep.* **2015**, *549*, 1-43.
21. Medeghini, F.; Crut, A.; Gandolfi, M.; Rossella, F.; Maioli, P.; Vallee, F.; Banfi, F.; Del Fatti, N., Controlling the Quality Factor of a Single Acoustic Nanoresonator by Tuning Its Morphology. *Nano Letters* **2018**, *18*, 5159-5166.
22. Devkota, T.; Brown, B. S.; Beane, G.; Yu, K.; Hartland, G. V., Making Waves: Radiation Damping in Metallic Nanostructures. *J. Chem. Phys.* **2019**, *151*, 080901.
23. Su, M. N.; Ostovar, B.; Gross, N.; Sader, J. E.; Chang, W. S.; Link, S., Acoustic Vibrations and Energy Dissipation Mechanisms for Lithographically Fabricated Plasmonic Nanostructures Revealed by Single-Particle Transient Extinction Spectroscopy. *J. Phys. Chem. C* **2021**, *125*, 1621-1636.
24. Lin, H. N.; Maris, H. J.; Freund, L. B.; Lee, K. Y.; Luhn, H.; Kern, D. P., Study of Vibrational Modes of Gold Nanostructures by Picosecond Ultrasonics. *J. Appl. Phys.* **1993**, *73*, 37-45.
25. Del Fatti, N.; Voisin, C.; Christofilos, D.; Vallée, F.; Flytzanis, C., Acoustic Vibration of Metal Films and Nanoparticles. *J. Phys. Chem. A* **2000**, *104*, 4321-4326.
26. Perner, M.; Gresillon, S.; März, J.; von Plessen, G.; Feldmann, J.; Porstendorfer, J.; Berg, K. J.; Berg, G., Observation of Hot-Electron Pressure in the Vibration Dynamics of Metal Nanoparticles. *Phys. Rev. Lett.* **2000**, *85*, 792-795.
27. Hu, M.; Wang, X.; Hartland, G. V.; Mulvaney, P.; Juste, J. P.; Sader, J. E., Vibrational Response of Nanorods to Ultrafast Laser Induced Heating: Theoretical and Experimental Analysis. *J. Am. Chem. Soc.* **2003**, *125*, 14925-14933.

28. Crut, A.; Maioli, P.; Del Fatti, N.; Vallee, F., Time-Domain Investigation of the Acoustic Vibrations of Metal Nanoparticles: Size and Encapsulation Effects. *Ultrasonics* **2014**, *56*, 98-108.
29. Ahmed, A.; Pelton, M.; Guest, J. R., Understanding How Acoustic Vibrations Modulate the Optical Response of Plasmonic Metal Nanoparticles. *ACS Nano* **2017**, *11*, 9360-9369.
30. Medeghini, F.; Rouxel, R.; Crut, A.; Maioli, P.; Rossella, F.; Banfi, F.; Vallée, F.; Del Fatti, N., Signatures of Small Morphological Anisotropies in the Plasmonic and Vibrational Responses of Individual Nano-Objects. *J. Phys. Chem. Lett.* **2019**, *10*, 5372-5380.
31. Saison-Francioso, O.; Lévêque, G.; Akjouj, A., Numerical Modeling of Acousto-Plasmonic Coupling in Metallic Nanoparticles. *J. Phys. Chem. C* **2020**, *124*, 12120-12133.
32. Krauss, T. D.; Wise, F. W., Coherent Acoustic Phonons in a Semiconductor Quantum Dot. *Phys. Rev. Lett.* **1997**, *79*, 5102-5105.
33. Vialla, F.; Del Fatti, N., Time-Domain Investigations of Coherent Phonons in Van Der Waals Thin Films. *Nanomaterials* **2020**, *10*, 2543.
34. Juvé, V.; Crut, A.; Maioli, P.; Pellarin, M.; Broyer, M.; Del Fatti, N.; Vallée, F., Probing Elasticity at the Nanoscale: Terahertz Acoustic Vibration of Small Metal Nanoparticles. *Nano Letters* **2010**, *10*, 1853-1858.
35. Xiang, D.; Wu, J.; Rottler, J.; Gordon, R., Threshold for Terahertz Resonance of Nanoparticles in Water. *Nano Letters* **2016**, *16*, 3638-3641.
36. Maioli, P.; Stoll, T.; Saucedo, H. E.; Valencia, I.; Demessence, A.; Bertorelle, F.; Crut, A.; Vallee, F.; Garzon, I. L.; Cerullo, G., et al., Mechanical Vibrations of Atomically Defined Metal Clusters: From Nano- to Molecular-Size Oscillators. *Nano Letters* **2018**, *18*, 6842-6849.

37. Martinet, Q.; Berthelot, A.; Girard, A.; Donoeva, B.; Comby-Zerbino, C.; Romeo, E.; Bertorelle, F.; van der Linden, M.; Tarrat, N.; Combe, N., et al., Performances of the Lamb Model to Describe the Vibrations of Gold Quantum-Sized Clusters. *J. Phys. Chem. C* **2020**, *124*, 19324-19332.
38. Rouxel, R.; Diego, M.; Medeghini, F.; Maioli, P.; Rossella, F.; Vallée, F.; Banfi, F.; Crut, A.; Del Fatti, N., Ultrafast Thermo-Optical Dynamics of a Single Metal Nano-Object. *J. Phys. Chem. C* **2020**, *124*, 15625-15633.
39. Major, T. A.; Crut, A.; Gao, B.; Lo, S. S.; Fatti, N. D.; Vallee, F.; Hartland, G. V., Damping of the Acoustic Vibrations of a Suspended Gold Nanowire in Air and Water Environments. *Phys. Chem. Chem. Phys.* **2013**, *15*, 4169-4176.
40. Ruijgrok, P. V.; Zijlstra, P.; Tchebotareva, A. L.; Orrit, M., Damping of Acoustic Vibrations of Single Gold Nanoparticles Optically Trapped in Water. *Nano Letters* **2012**, *12*, 1063-1069.
41. Yu, K.; Zijlstra, P.; Sader, J. E.; Xu, Q.-H.; Orrit, M., Damping of Acoustic Vibrations of Immobilized Single Gold Nanorods in Different Environments. *Nano Letters* **2013**, *13*, 2710-2716.
42. Chakraborty, D.; Sader, J. E., Constitutive Models for Linear Compressible Viscoelastic Flows of Simple Liquids at Nanometer Length Scales. *Phys. Fluids* **2015**, *27*, 052002.
43. Devkota, T.; Chakraborty, D.; Yu, K.; Beane, G.; Sader, J. E.; Hartland, G. V., On the Measurement of Relaxation Times of Acoustic Vibrations in Metal Nanowires. *Phys. Chem. Chem. Phys.* **2018**, *20*, 17687-17693.
44. Lermé, J.; Margueritat, J.; Crut, A., Vibrations of Dimers of Mechanically Coupled Nanostructures: Analytical and Numerical Modeling. *J. Phys. Chem. C* **2021**, *125*, 8339-8348.

45. Yu, K.; Major, T. A.; Chakraborty, D.; Devadas, M. S.; Sader, J. E.; Hartland, G. V., Compressible Viscoelastic Liquid Effects Generated by the Breathing Modes of Isolated Metal Nanowires. *Nano Letters* **2015**, *15*, 3964-3970.
46. Chakraborty, D.; Uthe, B.; Malachosky, E. W.; Pelton, M.; Sader, J. E., Viscoelasticity Enhances Nanometer-Scale Slip in Gigahertz-Frequency Liquid Flows. *J. Phys. Chem. Lett.* **2021**, *12*, 3449-3455.
47. Chakraborty, D.; van Leeuwen, E.; Pelton, M.; Sader, J. E., Vibration of Nanoparticles in Viscous Fluids. *J. Phys. Chem. C* **2013**, *117*, 8536-8544.
48. Yang, F.; Grimsley, T. J.; Che, S.; Antonelli, G. A.; Maris, H. J.; Nurmikko, A. V., Picosecond Ultrasonic Experiments with Water and Its Application to the Measurement of Nanostructures. *J. Appl. Phys.* **2010**, *107*, 103537.
49. Devkota, T.; Beane, G.; Yu, K.; Hartland, G. V., Attenuation of Acoustic Waves in Ultrafast Microscopy Experiments. *J. Appl. Phys.* **2019**, *125*, 163102.
50. Xu, F.; Guillet, Y.; Ravaine, S.; Audoin, B., All-Optical in-Depth Detection of the Acoustic Wave Emitted by a Single Gold Nanorod. *Physical Review B* **2018**, *97*, 165412.
51. Klieber, C.; Pezeril, T.; Andrieu, S.; Nelson, K. A., Optical Generation and Detection of Gigahertz-Frequency Longitudinal and Shear Acoustic Waves in Liquids: Theory and Experiment. *Journal of Applied Physics* **2012**, *112*, 013502.
52. Pezeril, T.; Klieber, C.; Andrieu, S.; Nelson, K. A., Optical Generation of Gigahertz-Frequency Shear Acoustic Waves in Liquid Glycerol. *Physical Review Letters* **2009**, *102*, 107402.

TOC graphic:



Biographies:



Kuai Yu received his Ph.D. in Physical Chemistry with Prof. Qing-Hua Xu at the National University of Singapore in 2013. He was then a postdoctoral researcher in Professor Hartland's group. In 2016, he started working at Shenzhen University, where he is currently an associate professor. His current research focuses on low-frequency acoustic phonon strong coupling in different types of acoustic resonators.



Yiqi Jiang received his B.S. degree in Optical Engineering from the Dalian University of Technology in 2020. He is currently studying for a master degree at Shenzhen University. His research interest is studying acoustic vibrations of single metal nanoparticles with time-resolved microscopy.



Cameron Wright received his B.S. degree in Chemistry from Butler University in 2019. He is currently pursuing a Ph.D. at the University of Notre Dame. His research interest lies in the development of time-resolved spectroscopy techniques to study the relaxation of single nanostructures.



Prof. Hartland obtained a Ph. D. from UCLA in 1991, and performed postdoctoral studies at the University of Pennsylvania with Prof. Hai-Lung Dai before joining the Department of Chemistry and Biochemistry at the University of Notre Dame in 1994. His research interests are in developing and applying novel spectroscopy techniques to study energy relaxation processes in single nanoparticles. Prof. Hartland is a Fellow of the AAAS, the American Chemical Society and the Royal Society of Chemistry.